Jour. Assoc. Expl. Geophys.
Oct. 1996, Vol. XVII No.4
pp 165 to 175

ESTIMATION OF STRUCTURAL GEOMETRY OF SATPURA CONDUCTIVITY ANOMALY THROUGH THE HILBERT TRANSFORMATION OF MAGNETOVARIATIONAL FIELDS

S.Y. Waghmare, B.R. Arora and Jana Pěčova*

Indian Institute of Geomagnetism, Colaba, Bombay - 400 005, India.
**Geophysical Institute, Czech Academy Sciences,*
Prague, Czech Republic.

Abstract

The magnetovariational data in horizontal and vertical field components recorded along a profile running across the SONATA and Satpura ranges are separated into its external and internal parts with an objective to decipher the configuration of anomalous currents associated with an elongated Satpura conductivity anomaly (SCA). The inferred distribution of anomalous internal currents approximate the SCA as an arcuate structure with its upper surface simulating asymmetric anticlinal geometry, in close agreement with the results of numerical modelling. In retrospective sense the results demonstrate that constraints provided by mapping the configuration of internal current distribution can be used as a guide on the choice of conductive structures to be investigated by modelling.

Introduction

Interpretational methods in magnetovariational (MV) studies, aimed at investigating the lateral electrical inhomogeneities in the earth's crust and upper mantle, require separation of transient geomagnetic field variations into parts of external and internal origin. Though formal techniques have been developed to effect the desired separation, they have rarely been implemented because fields of scale-lengths greater than the array size cannot be separated (see Gough and Ingham, 1983 for the review of techniques and their limitations). The problem, however, appears soluble for certain elongated (2-D) structures whose induction response exhibits wavelengths much smaller than the dimension of the array. In such cases, the integral formulae given by Siebert and Kertz (1957) can be applied to separate the observed fields into external and internal components. Adoption of this formulation to magnetovariational studies by calculating the Hilbert transform of horizontal and vertical fields defined along a profile perpendicular to the strike of the 2-D structure has been detailed by Pěčová (1982). She showed that resulting internal fields, corrected for the normal field, can be used to infer the horizontal location and the depth of the concentrated linear current, producing the anomaly, might flow. The application of this method on the data collected across the Carapathian had provided depth estimate of the Carapathian conductivity anomaly which agreed well with that indicated by numerical model fitting the frequency dependent transfer functions (Jankowski et al., 1977).

It may be recalled that faced with the difficulty of decomposing time-varying fields into external and internal components, much of the MV data processing proceeds with the separation of fields into normal and anomalous parts, analogous to the separation into regional and local parts practised in gravity and magnetic prospecting methods. In such a representation, normal part is the vector sum of the external field and its electromagnetic response in layered earth model for the region. The anomalous part is completely of internal origin and exists only if the medium has lateral inhomogeneity in conductivity. The transfer functions summarizing the relationship between anomalous and normal field components are the more commonly employed

Manuscript received : 12-06-95 ; accepted after revision : 09-08-95

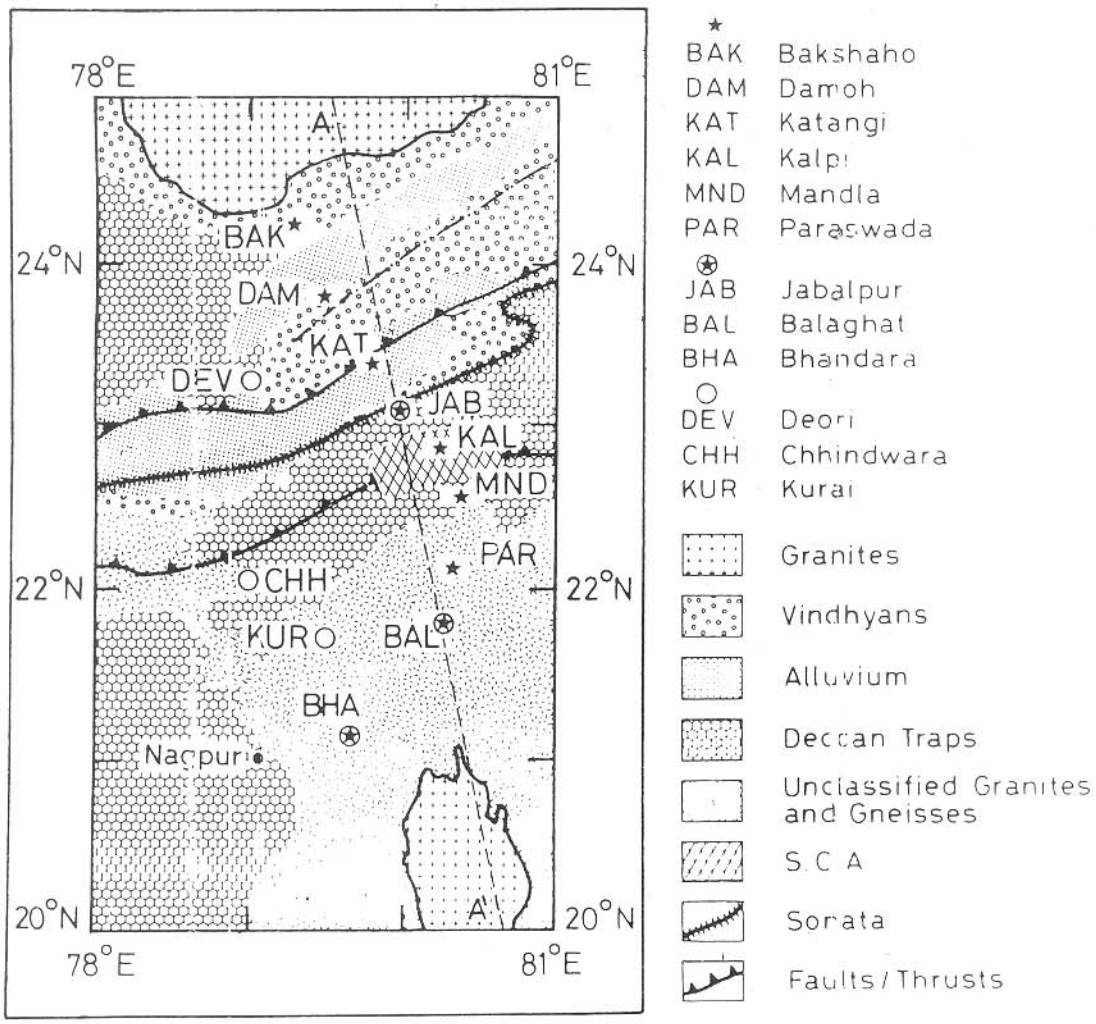

Fig. 1: Map of SONATA belt, Central India, showing locations of magnetometer sites (*) On the Bakshao-Mandla-Bhandara profile designed to map the Satpura Conductivity Anomaly (SCA), delineated earlier by regional magnetometer array (o). The line AA' marks transect, perpendicular to the strike of the SCA.

response functions useful in detecting and defining the anomalous internal currents (Schmucker, 1970). They also form important input functions in numerical modelling undertaken to define the geometry and electrical conductivity parameters of the mapped structure.

The present paper concerns with the application of the field separation technique, as refined by Pecová (1982), to the geomagnetic variational data collected from nine simultaneously operating field stations along the Bakshao-Mandla-Bhandara profile, central India, with an objective of mapping the geometry of the Satpura conductivity anomaly (SCA). The presence of an elongated conductive zone between the Jabhalpur-Balaghat sector of Satpura ranges was first revealed by a large-scale 2-D magnetometer array over central India, encompassing SONATA lineament bounded between 76 and 80 E (Arora et al., 1993). The reversal in the vertical field component, induction arrow pattern as well as polarization dependence of the anomalous fields were all diagnostic of an elongated conductive structure beneath the Satpura. However, the estimates on lateral

extent and depth were poorly constrained due to the large station-spacing. Therefore, a closely spaced profile (fig.1) was designed and operated to obtain spatially well resolved induction response so that more vigorous attempts could be made to model the parameters. The present exercise is a step towards this goal and is expected to supplement information obtained separately by processing data through more conventional technique of transfer functions, reported elsewhere (Arora et al., 1994).

Field Separation Procedure

The theoretical background of the method separating the observed variational field into external and internal parts, based on the formulation of Siebert and Kertz (1957), has been detailed in Pecova (1982). Some of the salient features and necessary steps are summarized in Appendix I to highlight its application to the present profile data. Given the spatial characteristic of transient horizontal (H) and vertical (Z) magnetic fields at any given instant of time along a profile perpendicular to the strike of involved conductor, the process of separation begins with the computation of Hilbert transform. Denoting the Hilbert transform of H and Z fields by KH and KZ respectively and using the subscript "e" for external and "i" for internal parts, the separation is obtained using the following simple relations:

$$H_e = \frac{1}{2}(H + KZ)$$

$$H_i = \frac{1}{2}(H - KZ) \quad \text{.....(1)}$$

$$Z_e = \frac{1}{2}(Z - KH)$$

$$Z_i = \frac{1}{2}(Z + KH)$$

.....(2)

Data Preparation

From a continuous string of time-varying magnetic field variations, sampled every one minute over a period of February-March, 1990, a number of disturbance events with simple waveforms were selected for the separation into external and internal parts. Such an example is shown in fig.2, where X

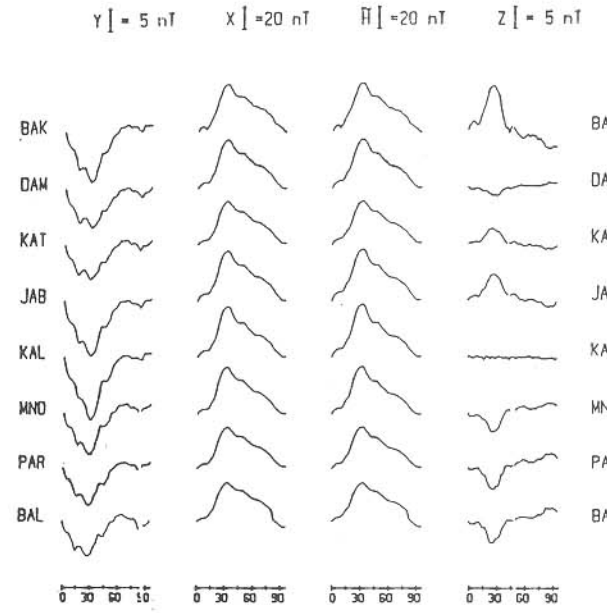

Fig. 2: An example of magnetovariational fields in north(X), east(Y) and vertical(Z) components. H -curve denote the sum of projected X and Y variation onto the direction of the profile.

(geographic north), Y (geographic east) and Z (vertical) components are stacked for an event recorded by eight stations. The large variability of Z variations including reversal of waveform on either side of KAL are definite diagnostic of concentrated flow of internal currents in a conductive structure, termed as the SCA. Further, the near zero-Z variations at KAL imply that centre of the SCA is in the close vicinity of KAL. The other Z reversals seen over the northern part of the profile are indicative of two other conductive zones, one with its centre located between KAT and DAM and second one placed between DAM and BAK. Given that variations at DAM and BAK are controlled by two other conductive zones, their data are not used in subsequent analysis here which focuses on mapping the geometry of the SCA.

Earlier examining induction arrow pattern and polarization dependence of induction response of the SCA, Arora et al. (1994) have reported that induction in the SCA maximizes when source field is polarized N 20° W while the orthogonal azimuth excites no response. Such behavior permitted them to infer that induction response of the SCA is compatible with an elongated 2-D structure striking N 70° E, thereby, justifying application of field

separation technique described in the Appendix. To comply with the assumption of the method about the field being two-dimensional, the horizontal field components (X and Y) were projected onto the direction of the profile aligned at right angles to the strike, marked as AA' on fig. 1. The nature of these transformed variations $\lambda(\widetilde{H})$ is also shown in fig. 2.

Application of Field Separation Method to the SCA

The $\widetilde{H}$ and Z for a given instant of time when plotted as a function of lateral position (x) of stations on the profile provide initial input data, $\widetilde{H}(x)$ and $Z(x)$, for calculating the Hilbert transform to effect separation of field through eqs. (1) and (2). Before subjecting the $\widetilde{H}(x)$ and Z(x) data sets to Hilbert transformation, it is necessary to specify physical bounds on the nature of normal field away from the anomalous zone. For instance, just above the region of anomalous body, embedded in a horizontally stratified medium, measured fields are the superposition of the normal and anomalous parts. Away from the anomalous region where conductivity varies only with depth and where the assumption regarding the quasi-uniform character of the external field appears justified, the vertical (Z) field would tend to be zero. Therefore, tapering of Z-field to zero baseline at distant locations on either side of the profile is consistent with this physical scenario. In the present case, judging from the spatial characteristic of Z(x) on the profile (fig.3), Z-fields were allowed to taper off to zero at distances of -110 km and 200 km, reckoned in relation to the location of KAL on the profile. By repeated processing, it was found that the length extend over which Z fields are made to taper off to zero does not affect the final depth estimates provided the section of the profile where anomalous fields are strong is used in the preparation of hodographs, described later. In contrast to the Z variation, the constituents of the normal field components being additive in nature, $\widetilde{H}(x)$ field does not vanish away from anomalous zone and even constitutes large fraction of H in the anomalous domain. In such a situation, the field recorded at the station farthest from the anomalous zone (southern most station in the present case) was reckoned to be the measure of normal field. Only the difference between the $\widetilde{H}$ (x) recorded at each station on the profile and the field recorded at the reference site,

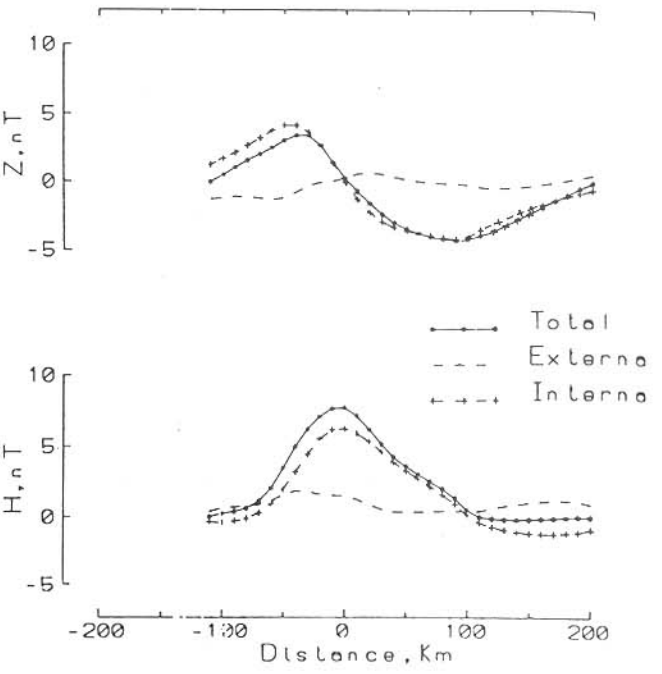

Fig. 3: The input functions in H and Z together with decomposed external (H_e , Z_e) and internal (H_i , Z_i) field components along the profile.

after suitably decreasing to zero at northern end, were used for Hilbert transformation. The procedure is equivalent to the practice adopted to separate the field into normal and anomalous parts, required for the estimation of transfer functions. If the reference station was really 'normal', the residual (anomalous) field at other stations could be directly used to estimate depth of the anomalous body using Z/Ha ratios. (Summers, 1981, Beamish 1987). The present method has the advantage that distribution of the internal components of the field along the profile can be obtained without assuming a constant external field over the entire length of the profile.

The values of $\widetilde{H}$ and Z distributed irregularly along the profile, were interpolated onto a regular spacing using quasi-Hermite splines which have the property of being continuous with a continuous first derivative. As elaborated above, these smooth continuous values were cut off by zero values of the field component at two fictitious locations placed on either sides of anomalous block, far enough from its centre. These uniformly grided field values in $\widetilde{H}$ and Z were then used to calculate Hilbert transform through Fourier transformation, exchanging the real and imaginary parts (with the necessary sign

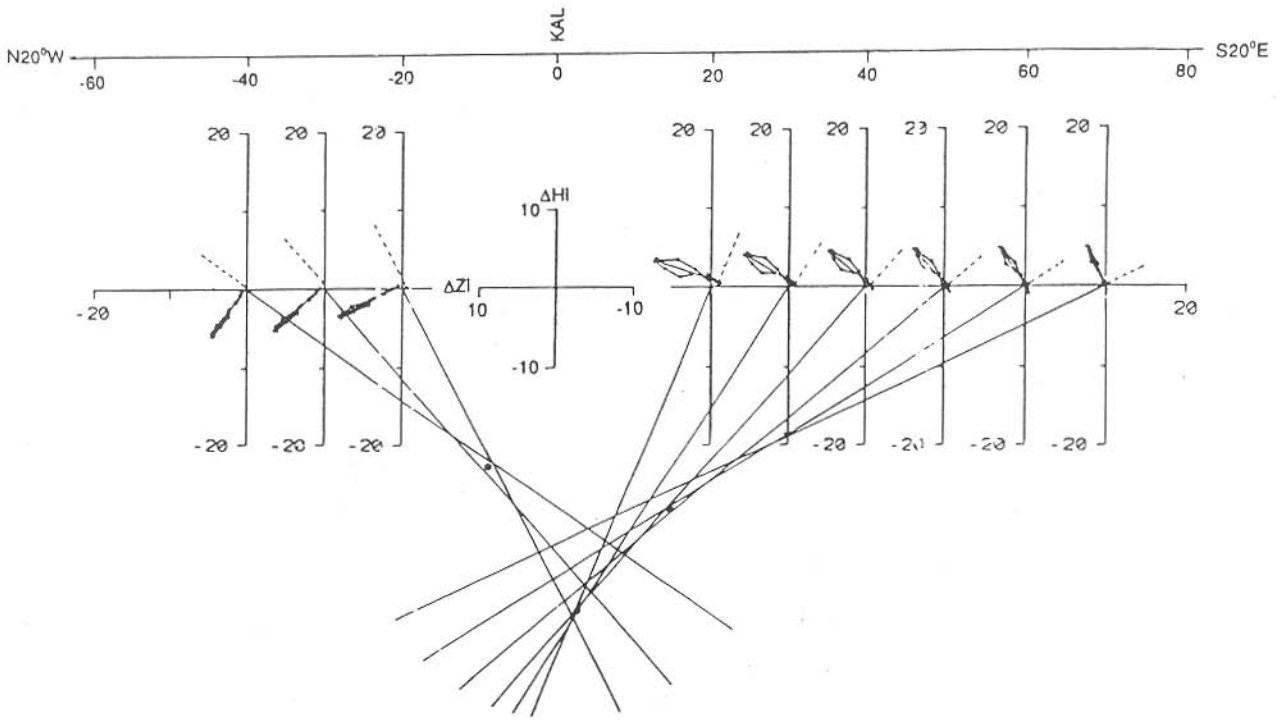

Fig. 4: Hodographs of H_i - Z_i at different locations along the profile AA'. Intersection points of normals to the H_i - Z_i vectors, drawn from different locations, provide co-ordinates of the current axis causing internal fields.

convention), and inverse Fourier transformation. Substituting these in equations (1) and (2) external and internal parts were obtained at specific locations along the profile. It must be emphasized the direction of the profile is important in the ensuing calculations. If the profile is directed in the direction of positive H component (i.e. northward or NW), the resulting Hilbert transform ($K\tilde{H}$ and KZ) can be directly substituted in equations (1) and (2) for the separation of components. However, when profile runs from north to south (or NW-SE), the sign of $K\tilde{H}$ and KZ is required to be reversed before substitution. Fig.3 gives example of the separated external and internal fields together with the input function corresponding to the time instant of peak value in fig.2.

Estimation of Geometry of Anomalous Current Distribution

The procedure is repeated for several instants of time of the disturbance event. The resulting H_i and Z_i for a series of instants are then used to define the hodograph in the Z - H plane at different locations along the profile (fig.4). The depth of a common source in the form of a concentrated linear current producing the anomalous internal fields could then be provided by the point of intersection of the normal to the vector defined by H_i and Z_i at certain locations along the profile. Physical essence of this simple approach follows from the fact that magnetic field lines associated with the line-current flowing along the y-axis of a orthogonal coordinate system would be represented by concentric circles in x-z plane. In such a case, disturbance vector defined by H_i and Z_i marks the tangent to the lines of force cutting the surface of the earth at the measuring site. Normal to this tangent at two or more sites along the profile will uniquely determine the depth and lateral position of the line current producing the magnetic fields.

Figure 4 demonstrates the examples of the graphical estimation of the depth of the source current using variational fields shown in fig.2. To obtain the depth estimate of the anomalous body we need to use only anomalous internal field component (H_i

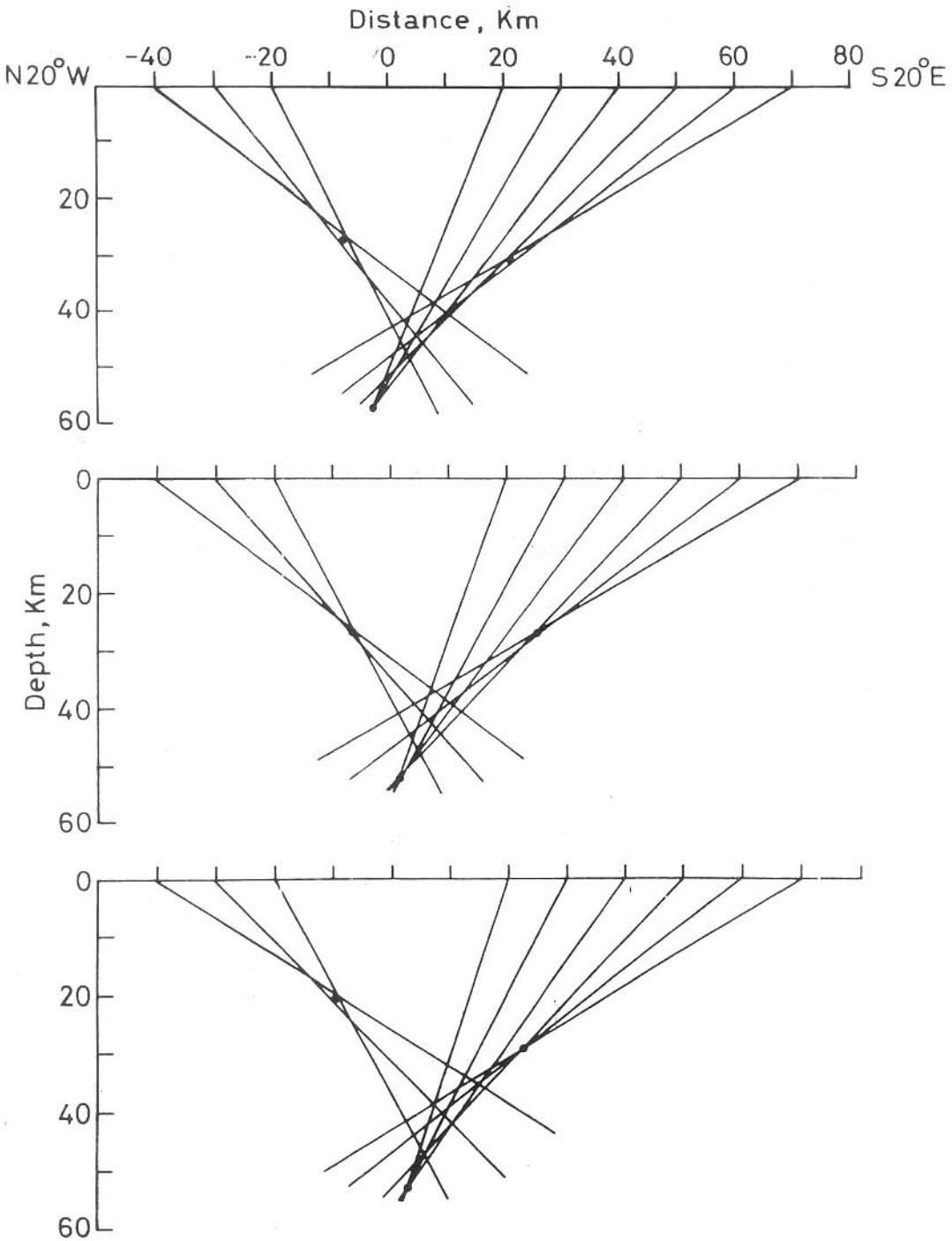

Fig. 5: Normals to the H_i - Z_i plane from different locations along the profile for three isolated disturbance events. The normals define three distinct zones of intersections, approximately at depths of 25, 55 and 30 km with their lateral position roughly placed at -5, 5 and 15 km with respect to location of KAL on the profile.

anomalous = H_i – H_i normal), therefore a correction in respect of the normal internal field was applied to all isolated H_i values. Here again, the value of H_i at the southernmost site was taken to be the measure of H normal. No correction was required to be incorporated with Z component because entire Z

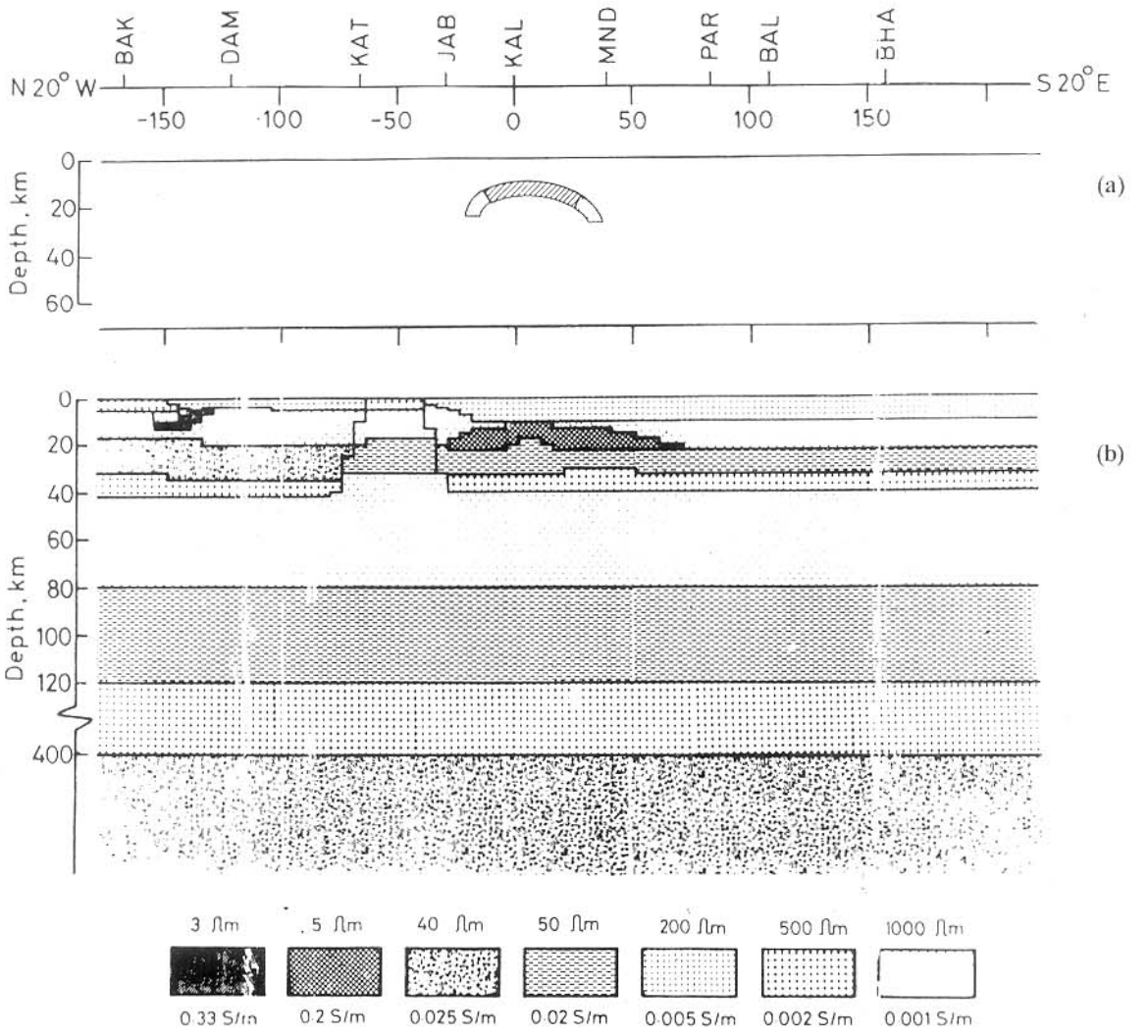

Fig.6 a): Inferred cross-section of the Satpura Conductivity Anomaly (SCA) in a vertical plane across the strike. The body is composed of three arcuate-shaped segments with their centres, shown by solid dots, at the intersection points located in Fig. 5

b): Geometry of the SCA (cross hatched zone) obtained by 2-D numerical modelling (Arora et al., 1994).

is attributed to induction in anomalous body. The magnitude of the correction in respect of regional H_i was only marginal because bulk of the normal $\tilde{H}$ field was subtracted prior to separation procedure. It can be seen that the graphical method locate the depth and lateral position of equivalent line current with considerable scatter (probable causes are discussed later).

The method of field separation was extended to several disturbance events. The results obtained from three events of varied morphology, lasting from 60 to 100 minutes are presented graphically in fig.5. For the clarity of the presentation, only normals to the $H_i - Z_i$ vectors are shown.

Results and Discussion

As described earlier, the intersection of the normals is expected to define the position of the equivalent-line current causing the anomaly. In the first instance, it must be realized that the assumption of the linear electric current is certainly only a first

order approximation to an elongated geological structure causing concentration of induced currents. As can be seen in Figures 4 and 5 the intersections are obtained with a large degree of scatter, both vertically and laterally, perhaps, pointing that the actual distribution of anomalous currents is far more complex than that can be approximated by a linear current. A more critical examination of Figures 4 and 5 reveals that despite large scatter in intersection points certain coherent pattern can still be recognized which persists in different disturbance events analyzed (fig.5). One finds that normals drawn from the locations situated on the NW part of the profile intersect at relatively shallow depth, ranging between 20-30 km. In comparison the normals from SE sector for surface positions located between 20-40 km SE of KAL intersect at much greater depths than the normals drawn from locations between 40-70 km. The centres of these three distinct zones of intersections are estimated to lie at average depths of 25, 55 and 30 km, based on the results shown in fig.5. The intersection zones, often seen as triangular area (centre marked by solid dots in fig.5), also show marked lateral shifts in their central location. The lateral position of these intersections, on average, are estimated to be at a distance of -5, 5 and 15 km in relation to the location of KAL on the profile.

Some of the above notable features can be reconciled if we assume that in the vertical cross-section across the strike, different segments of the SCA conductive structure have arcuate shape with different radii of curvature. In fig.6a, we attempt to trace the possible cross-section of the structure in a vertical plane across the strike . The structure is visualized to be composed of three arcs of finite thickness located at some arbitrary depths. The induced currents directed at right angles to each segment give rise to surface magnetic fields equivalent to a line current placed at the central coordinates of the intersection zones, which also form the centre of the arcs defining the body. Fig.6b shows the geometry of the SCA (hatched zone), as approximated by numerical modelling (Arora et al., 1994). It is rather striking that in geological sense the overall geometry of the conductive zone, as inferred by two independent approaches, can be viewed as an arcuate structure with its top exhibiting asymmetric anticlinal geometry.

The probable explanation for the enhanced conductive zone and its correlation with other geophysical data have already been discussed in Arora et al. (1994). It is not intended to repeat these aspects here but it is worthy of note that inferred arcuate nature of the mapped SCA is consistent with the tectonic scenario of the Satpura ranges which have often been interpreted as an uplifted horst following the crustal doming (Sethna, 1974). It is also pertinent to note that area of the SCA is marked by geothermal anomaly (Ravi Shanker, 1991) and correlates with the well-known Mandla gravity high (NGRI gravity map, 1975). In agreement with the evidence for a high velocity layer at mid-crustal depth, Mall et al., (1991) and Mishra (1992) interpreted the gravity high in terms of a local magmatic body at mid-crustal depths. The collocation of gravity, seismic velocity , conductivity and geothermal anomalies, all confined to restricted area rather than extending over the entire length and breadth of the Satpura ranges, in reasonable probability indicates that all anomalies may be different manifestation of a localized tectonic activity in this part of the Satpura range. One possible scenario visualized in earlier paper included emplacement of secondary silicic magma pond at mid-crustal depths in association with Deccan trap volcanism. As the magma pond cooled to ambient temperature, it would have a higher density and seismic velocity as revealed. Hydrous fluids released from crystallizing magmatic body or metamorphic fluids generated by dehydration reactions (Stanley et al., 1990) could be the potential source contributing to the high conductivity of the SCA. Alternatively, the body could have concentration of highly conductive minerals from the mantle, e.g. grain boundary films of carbon could be the potential candidate (Frost et al., 1989) . The presently available geophysical signatures, however, do not permit discrimination between graphite or free fluid sources for the mapped SCA.

Conclusions

The application of the field separation technique to magnetovariational data set over a known anomaly, convincingly demonstrates the efficacy of the method to map complex conductivity structure, although initially method was thought to provide only simplified model of the conductivity anomaly as a linear conductor. The high degree of correspondence of the inferred geometry with the results

of numerical modelling warrant that estimation of internal current distributions by the method of field separation, at the initial stage of data processing, can be helpful in restricting the range of structures to be investigated by numerical modelling.

Acknowledgements

The authors wish to thank Dr. G.K. Rangarajan for many simulating discussions. The cooperation received from Mr. M.V. Mahashabde in data collection and reduction is deeply appreciated. Authors thank Prof. B.P. Singh, Director, IIG for his encouragement. Financial grants received from Department of Science and Technology, Govt. of India, under their scheme on "Deep Continental Studies in India" is acknowledged with thanks.

References

Arora, B.R., Kaikkonen P, Mahashabde, M.V. and Waghmare S.Y., 1993, Phys. Earth Planet. Intr. 81, 201-213.

Arora B.R., Waghmare S.Y. and Mahashabde M.V., 1994, *Geomagnetic depth sounding along the Hirapur-Mandle-Bhandara profile, central India*, Mem. Geol. Soc. India (in press).

Beamish D., 1987, *A simple function for mapping induced currents*, Geophys. J.R. astr. Soc., 90, 485-494.

Frost B.R., Fyfe W.S., Tazaki K. and Chan T., 1989, *Grain-boundary graphite in rocks and impication for high electrical conductivity in the lower crust,* Nature, 340, 134-136.

Gough D.I. and Ingham M.R., 1983, *Interpretation methods or magnetometer arrays,* Rev. Geophys., 21, 805-827.

Jankowski J., Szymanski, Pec K., Cerv V., Petr V., Pecova J. and Praus O., 1977, *Anomalous Induction in the Carpathians,* Studia geoph. et. geod. 21, 35-57.

Mall D.M., Kaila K.L. and Rao V.K, 1991, *Magmatic body interpreted at mid-crustal level between Jabalpur and Mandla as an indicator for one of the source regions for Deccan Basalt,* Proc., First Int. Sym & Exhibition on "Exploration Geophysics in Nineteen Nineties" AEG, Hyderabad, Nov. 25-30, 1991, 1, 298-303.

Mishra D.C., 1992, *Mid-continent gravity high of central India and the Gondwana tectonics,* Tectonophysics, 212, 153-161.

NGRI Gravity map series of India, GPH-4 1975.

Pecová. J., 1982, *Determination of the depth of a conductivity anomaly by separating the geomagnetic variation field into its external and internal parts,* Travaux Geophysiques, XXX , 175-197.

Ravi Shanker, 1991, *Thermal and crustal structure of 'SONATA'. A zone of mid-continental rifting in Indian shield,* J. Geol. Soc. India, 37, 212-220.

Siebert M. and Kertz W., 1957, *Zur Zerlegung eines lokalen erdmagnetischen Feldes in ausseren und inneren Anteil, Nachr, Akad,. Wiss, Gottingen,* Math-Phys. 1 Abt. II a, 87.

Schmucker U., 1970, *Anomalies of geomagnetic variations in the southwestern United States,* Bull. Scripps Inst. Oceanogr., 13, 1-165.

Sethna, S.R., 1974,*Geochemistry of the Precambrian alkaline rocks and carbonatites of India-gaps in our knowledge,* J. Geol. Soc. India, 15, 429-433.

Stanley W.D., Mooney W.D. and Fuis G.S., 1990, *Deep crustal structure of the Cascade range and surrounding regions from seismic refraction and magnetotelluric data,* J. Geophy. Res., 95, 19419-19438.

Summers D.M., 1981, *Interpreting the magnetic fields associated with two-dimensional induction anomalies,* Geophys. J.R. astr. Soc., 65, 535-552.

Appendix I

Theoretical background of the method for the decomposition of magnetovariational fields into external and internal parts:

For a 2-D case, where the conductivity is uniform everywhere parallel to the strike (y-axis) and varies only vertically (z-axis) and horizontally along a profile running perpendicular to the strike (x-axis) of the conductivity structure, the Laplace's equation can be written as

$$\frac{\delta X}{\delta x} + \frac{\delta Z}{\delta z} = 0 \; ; \; \frac{\delta Y}{\delta y} = 0 \qquad \text{.....(1)}$$

Thus along the profile

$$\Delta V = \frac{\delta^2 X}{\delta x^2} + \frac{\delta^2 Z}{\delta z^2} = 0 \qquad \text{.....(2)}$$

Expressing the variable $V = U(x)\, W(z)$, leads to the particular solution for $\omega > 0$.

$$V = \exp(i\omega x \pm \omega z)$$
$$= \exp(i\omega x)\, \exp(\pm \omega z)$$
$$= \left\{ \begin{matrix} \cos \\ \sin \end{matrix} \right\} (\omega x)\, \exp(\pm \omega z) \qquad \text{.....(3)}$$

When integrated with respect to the parameter ω (frequency of the spatial distributon of the field), eq. (3) yields a more general solution to Laplace's eq. The potential V of the observed magnetic field is composed of two parts, $V = V_i + V_e$

After integrating eq. (3) w.r.t. ω, the expression for the internal and external parts of the potential, V_i and V_e, can be arrived at as follows

$$V_i = \int_0^\alpha [a_i(\omega) \cos(\omega x) + b_i(\omega) \sin(\omega x)] \exp(\omega z)\, d\omega \qquad \text{for } z \geq 0$$

$$V_e = \int_0^\alpha [a_e(\omega) \cos(\omega x) + b_e(\omega) \sin(\omega x)] \exp(-\omega z)\, d\omega \qquad \text{for } z \leq 0$$

At the earths surface, $z = 0$, the vertical component $Z(x)$ and the horizontal component $H(x)$, can be derived from V as follows

$$Z(x) = (-\delta V/\delta z)_{z=0} = \int_0^\alpha \omega[(-a_1 + a_e)\cos(\omega x) + (-b_1 + b_e)\sin(\omega x)]\, d\omega$$

$$H(x) = (-\delta V/\delta z)_{z=0} = \int_0^\alpha \omega[-(b_1 + b_e)\cos(\omega x) + (a_1 + a_e)\sin(\omega x)]\, d\omega \qquad \text{.....(5)}$$

Siebert and Kertz (1957) introduced a linear operator K, termed Kertz operator, defined below to facilitate evaluation of eq.(4) and its decomposition into external and internal parts. For a function

$$f(x) = \int_0^\alpha [a(\omega)\cos(\omega x) + b(\omega)\sin(\omega x)]\, d\omega \qquad \text{.....(6)}$$

the product

$$Kf(x) = \int_0^\alpha [-b(\omega)\cos(\omega x) + a(\omega)\sin(\omega x)]\, d\omega \qquad \text{.....(7)}$$

$$H_e(x) = \int_0^\alpha \omega[-b_e(\omega)\cos(\omega x) + a_e(\omega)\sin(\omega x)]\, d\omega$$

$$Z_e(x) = \int_0^\alpha \omega[a_e(\omega)\cos(\omega x) + b_e(\omega)\sin(\omega x)]\, d\omega \qquad \text{.....(8)}$$

In terms of Kertz operators, eq(8) reduces to

$$H_e(x) = KZ_e(x), \quad H_e(x) = -K Z_i(x) \qquad \text{.....(9a)}$$

Since $K(Kf) = K^2 f = -f$,

$$KH_e(x) = -Z_e(x), \quad KH_i(x) = Z_i(x) \qquad \text{.....(9b)}$$

With the aid of eqs. (9a) and (9b), the observed fields in H(x) and Z(x) can be seperated into its constituents

Expressing $H(x) = H_e(x) + H_i(x)$
and $KZ(x) = K[Z_e(x) + Z_i(x)] = H_e(x) - H_i(x)$

we obtain

$$H_e(x) = 1/2\,[H(x) + KZ(x)] \qquad \text{.....(10a)}$$

$$H_i(x) = 1/2\,[H(x) - KZ(x)] \qquad \text{.....(10b)}$$

Similarly for $Z(x) = Z_e(x) + Z_i(x)$

and $KH(x) = K[H_e(x) + H_i(x)]$

$= - Z_e(x) + Z_i(x)$

we get

$$Z_e(x) = 1/2 [Z(x) - KH(x) \quad \text{.....(11a)}$$

$$Z_i(x) = 1/2 [Z(x) + KH(x) \quad \text{.....(11b)}$$

Pecová (1982) showed that if operator K can be further expressed as an integral operator, the coefficients of Fourier's transformation

$$\begin{Bmatrix} a(\omega) \\ b(\omega) \end{Bmatrix} = \frac{1}{\pi} \int_{-\alpha}^{+\alpha} f(\xi) \begin{Bmatrix} \cos \\ \sin \end{Bmatrix} (\omega\xi)\, d\xi \quad \text{.....(12)}$$

eq.(7) can then be expressed as

$$Kf(x) = \int_0^{\alpha} [-b(\omega) \cos(\omega x) + a(\omega) \sin(\omega x)]\, d\omega$$

$$= \int_0^{\alpha} d\omega \; 1 \int_{-\alpha}^{+\alpha} f(\xi) [-\sin(\omega\xi) \cos(\omega x) + \cos(\omega\xi) \sin(\omega x)] d\xi \quad \text{.....(13)}$$

By definition of the improper integral

$$Kf(x) = \lim_{\Omega \to \alpha} \frac{1}{\pi} \int_{-\alpha}^{+\alpha} f(\xi)\, d\xi \int_0^{\Omega} \sin\omega(x - \xi)\, d\omega \quad \text{.....(14)}$$

The second integral of eq.(14) can be further expressed as

$$\int_0^{\Omega} \sin\omega(x-\xi)\, d\omega = Im \int_0^{\Omega} \exp(i\omega X')d\omega \text{ for } x - \xi = X' \quad \text{.....(15)}$$

Multiplying eq.(15) by the convergence factor $\exp(-e\omega)$ and evaluating the integral as well as its limits, it can be shown that

$$\lim_{\Omega \to \alpha} \int_0^{\Omega} \sin\omega(x-\xi)d\omega = \lim Im \int_0^{\Omega} \exp(i\omega X')d\omega = \frac{1}{X'} = \frac{1}{x-\xi} \quad \text{.....(16)}$$

Introducing this simplification, eq.(14) finally reduces to

$$\lim_{\Omega \to \alpha} \frac{1}{\pi} \int_{-\alpha}^{+\alpha} f(\xi)d\xi \int_0^{\Omega} \sin\omega(x-\xi)d\omega = Kf(x) = \frac{1}{\pi} \int_{-\alpha}^{+\alpha} f(\xi) \frac{1}{x-\xi} d\xi \quad \text{.....(17)}$$

It can be seen that right hand side is a hilbert transformation of function $f(\xi)$.

Extending the analogy, the magnetic field variations H(x) and Z(x) observed at the earth's surface (z = 0) along the profile perpendicular to the strike of 2-D structure can then be used to calculate KH(x) and KZ(x), which when substituted in eqns. (10) and (11) yield external and internal parts in respective field components.